Scientific Reports

https://doi.org/10.1038/s41598-026-38034-4

Article in Press

Comparative analysis of microRNA expression in serum-derived extracellular vesicles from sudden infant death syndrome cases

Received: 27 September 2025

Accepted: 28 January 2026

Published online: 10 February 2026

Cite this article as: Kanno S., Fukuta M., Kato H. *et al.* Comparative analysis of microRNA expression in serum-derived extracellular vesicles from sudden infant death syndrome cases. *Sci Rep* (2026). https://doi.org/10.1038/s41598-026-38034-4

Sanae Kanno, Mamiko Fukuta, Hideaki Kato, Jun Monma-Otaki, Yoshimi Nakamura & Toru Oshima

Comparative analysis of microRNA expression in serum-derived extracellular vesicles from sudden infant death syndrome cases

*Sanae Kanno[1], Mamiko Fukuta[1, 2], Hideaki Kato[1], Jun Monma-Otaki[1], Yoshimi Nakamura[1], Toru Oshima[1]

[1] Department of Forensic Medicine, Nagoya City University Graduate School of Medical Sciences, Nagoya, Japan

[2] Department of Legal Medicine, Aichi Medical University School of Medicine, Nagoya, Japan

*Correspondence should be addressed to: Sanae Kanno, Ph.D.

ORCID ID: 0000-0001-6415-7777

Department of Forensic Medicine, Nagoya City University Graduate

School of Medical Sciences,

1 Kawasumi, Mizuho-cho, Mizuho-ku, Nagoya 467-8601, Japan

Tel: +81-52-853-8180

E-mail: sanae@med.nagoya-cu.ac.jp

ABSTRACT

Sudden infant death syndrome (SIDS) remains one of the most common and poorly understood diagnoses of death in infants. In this study, we searched for novel biomarkers to aid in elucidating the pathogenesis of SIDS through a bioinformatics analysis of serum-derived extracellular vesicle (EV) miRNAs using next-generation sequencing. Comparative analyses between infants who died of SIDS and those who died from known causes showed that 15 and 38 miRNAs were significantly up- or down-regulated more than 2-fold in SIDS, respectively. Myocardial-specific miRNAs, such as miR-1, miR-208, and miR-499, which are known to leak from injured heart, were up-regulated markedly in SIDS EVs. Gene target prediction analyses suggested that the MAP signaling pathway, cardiomyocytes, and cardiac ion channels are involved in the pathogenesis of SIDS. Gene ontology analyses revealed that protein phosphorylation, the actin cytoskeleton and myosin complex, and kinase activity are heavily involved in SIDS. Our results indicate that EV myocardial-specific miRNAs are released into the blood from the heart in SIDS, suggesting the pathogenesis of SIDS is associated with cardiac injury. Studies of EV miRNAs using minimally invasive fluid samples could lead to the discovery of new diagnostic markers for SIDS.

Keywords

Sudden infant death syndrome / Extracellular vesicles / MicroRNA / Comparative analysis / Next-generation sequencing

INTRODUCTION

Sudden infant death syndrome (SIDS) is defined as "the sudden and unexpected death of an infant under 1 year of age, which remained unexplained even after a complete investigation, including performance of a complete autopsy". Although the incidence of SIDS has been decreasing due to safe sleep campaigns, it remains a leading cause of postmortem infant death in developing and even developed countries [1]. Despite decades of investigation, however, the exact causes of SIDS remain largely unknown due to the complex nature of etiology. Unlike other syndromes, no consistent and reproducible diagnostic tissue markers or pathognomonic markers of SIDS notable on autopsy are available. Furthermore, SIDS is extremely difficult to diagnosis because affected infants have died by the time of diagnosis. Therefore, novel diagnostic markers for SIDS are urgently needed.

Recent studies have shed light on biological markers that could be linked to an increased risk of SIDS, including markers of immune responses and autonomic dysfunction [2-4]. Numerous epidemiological and physiological factors associated with an increased risk of SIDS have been identified; however, these factors are too generic for precise identification of high-risk infants. The most accepted theory of the pathogenesis of SIDS involves a complex interaction described by the "Triple Risk Model", which consists of "a vulnerable infant, a predisposing factor, and an exogenous stress", rather than simple cause [5,6]. The final mechanism of SIDS is thought to involve a combination of immature cardiorespiratory control and a failure of arousal resulting from defects in the brainstem [7]. Cohort studies have attempted to identify genetic factors that may predispose infants to SIDS. Genetic predisposition most likely involved a polygenic inheritance pattern—a combination of gene variants and polymorphisms that combine to increase susceptibility [8,9]. Although many genetic alterations have been linked to SIDS, the genetic contribution remains unclear.

Extracellular vesicles (EVs), which are endogenous nano-sized (40-150 nm) vesicles, carry a variety of functional molecules, including messenger RNA (mRNA), microRNA (miRNA), DNA, lipids, and proteins [10]. Depending on the pathological and physiological state of a tissue, EVs may rapidly transfer these molecules from host cells to recipient cells via biological fluids, such as blood, urine, saliva, bronchoalveolar lavage fluid, or milk [11]. EVs function as pivotal mediators of cell-to-cell communication and contribute to the pathogenesis of many diseases. miRNAs are small (~20–23 nucleotides in length), non-coding RNAs that regulate target gene expression at the post-transcriptional level [12]. Current research suggests that EV miRNAs could be suitable non-invasive biomarkers of a number of human diseases, including various cancers, cardiovascular disease [11,13], and neurodegenerative diseases [14]. Postmortem changes such as blood coagulation and RNA and DNA degradation progress in cadavers over time. However, we previously reported that EVs and their contents are protected from degradation by RNases and can remain in a very stable state even in cadaver fluids because they are encapsulated by a lipid bilayer membrane. Furthermore, analyses of serum EV miRNAs from cadavers of individuals who died of acute myocardial infarction (AMI) identified disease-specific miRNA expression patterns consistent with those detected in clinical diagnoses [15]. These results suggest that the pathological processes that lead up to death from SIDS could be elucidated by analyzing cadaver fluid samples. As fluids such as blood or urine can only be obtained at autopsy in cases of SIDS, there is great interest in identifying EV miRNAs in minimally invasive fluid samples that would be useful for SIDS diagnosis.

To identify markers of SIDS risk and pathological changes that precede death by SIDS, we performed comparative analyses of serum-derived EV miRNAs from infants deceased due to SIDS versus non-SIDS causes using next-generation sequencing (NGS). The goal of this study was to elucidate the complex mechanism of death by SIDS and identify specific markers for SIDS using small amounts of less-invasive samples.

RESULTS

Autopsy cases

Table 1 summarizes the case profiles.

Characterization of EVs

EVs were characterized based on western blotting, size distribution, and morphology. Measurement of EV size distribution using both dynamic light scattering (DLS) (Fig. 1A) and scanning electron microscopy (SEM) observation (Fig. 1B) showed that approximately 90% of the vesicles in serum had an average diameter of 200 nm. As shown in Figure 1C, the common EV marker proteins CD9 and CD63 were present in abundance in the lysate of serum-derived EVs. CD63, a glycoprotein, was detected as a smeary 30- to 60-kDa band of glycosylated protein. Uncropped western blots are shown in Supplemental Figure 1. These results indicate that the method provides for highly efficient EV isolation.

RNA quality

The quality of EV RNA was assessed based on Bioanalyzer electropherograms. EV RNA exhibited a sharp peak of approximately 25 nucleotides (Fig. 2). No notable differences were observed in peak patterns among samples. Sufficient amounts of small RNA could be extracted for NGS analysis.

Overview of small RNA NGS data

NGS of EV miRNA expression yielded an average of 12.1 million reads per samples (Table 2). The average percentage of clean reads on the tags was 96.8%, with even the least clean sample achieving 86.4%. On average, >98% of bases were output as Q30, indicating the

analysis was highly accurate.

Analysis of overlap in differentially expressed miRNAs between infants who died of SIDS and control (CT) infants who died of known causes

Overlapping and group-specific differentially expressed miRNAs were shown in a Venn diagram (Fig. 3A), volcano plot (Fig. 3B), and miRNA expression profile heat map (Fig. 3C). The Venn diagram indicated that 81 and 7 miRNAs were expressed in SIDS and CT samples, respectively. As shown in the volcano plot, a total of 15 miRNAs were significantly up-regulated and 38 miRNAs significantly down-regulated in SIDS compared with CT. A list of miRNAs significantly up- or down-regulated at least 2-fold, excluding those with a read count of ≤5 in both SIDS and CT samples, is shown in Table 3. These miRNAs included miR-1, miR-208, and miR-499-5p, which are specifically present in cardiac and skeletal muscle and known as myocardial abundant miRs (myo-miRs). It is noteworthy that myo-miRs such as miR-1, miR-208, and miR-499 were up-regulated in SIDS. By contrast, 38 miRNAs including miR-122-5p and miR-192-5p were down-regulated in SIDS. The miRNA heat map revealed that the pattern of EV miRNA expression tended to differ between SIDS (right 4 columns) and CT (left 4 columns).

Gene Ontology (GO) functional and Kyoto Encyclopedia of Genes and Genomes (KEGG) pathway enrichment analyses of EV miRNAs

GO and KEGG analyses [16] were performed to investigate the biological processes, specific molecular functions, and related signaling pathways associated with differentially expressed miRNAs. The GO functional analysis shows that protein phosphorylation in biological process, actin cytoskeleton and myosin complex in cellular component, and kinase activity in molecular

function play significant roles in SIDS (Fig. 4A and 4B).

KEGG pathway enrichment analysis was performed to identify pathways significantly involved in SIDS. The analysis revealed that the mitogen-activated protein kinase (MAPK) and Ras signaling pathways are significantly associated with the pathophysiology of SIDS (Fig. 5A). Among all set collections enriched in SIDS within the KEGG database, genes tended to decrease overall. Therefore, we focused on the five most significant pathways in SIDS. The resulting gene set enrichment analysis suggested that SIDS involves a core enrichment of genes associated with cardiac muscle contraction (Fig. 5B) and a decrease in genes associated with cardiac ion channels in cardiomyocytes. Genes such as dihydropyridine receptor (DHPR), Na^{+}/Ca^{2+} exchanger (NCX), ATP, junctin (JCN), myosin, and sarcoplasmic/endoplasmic reticulum Ca^{2+}ATPase 2a (SERCA2a) were down-regulated in SIDS compared with CT (Fig. 5B). Furthermore, genes related to calcium signaling pathways (Fig. 5C) and adrenergic signaling in cardiomyocytes (Fig. 5D) also appeared to be modulated in SIDS. Figure 5E showed that MAPK pathway-related genes, except hematopoietic progenitor kinase 1 (HPK1), MAP 3 kinase 4 (MEKK4), and FAS, are markedly down-regulated in SIDS. Furthermore, similar to the results shown in Figure 4A, genes associated with pathways affecting the actin cytoskeleton were down-regulated in SIDS (Fig. 5F).

DISCUSSION

To our knowledge, this is the first study to utilize EVs to identify useful markers for diagnosis of SIDS and elucidating its pathogenesis. We performed comparative analyses of miRNA expression in serum-derived EVs of samples obtained from SIDS and CT infants. The comparison of EV miRNA expression showed that 15 miRNAs were significantly up-regulated in SIDS (Fig. 3B). Surprising, several myo-miRs, including miR-1, miR-208, and miR-499-5p,

were up-regulated in SIDS (Table 3). These myo-miRs are rapidly released and carried via EVs to the peripheral blood in abundance after cardiac injury, such as AMI [17], and have therefore been reported as potential biomarkers of AMI [18-21]. Our results suggest that the changes leading to SIDS-related death might be due to pathophysiological changes similar to those that occur during heart failure.

We were able to find only one study reporting SIDS-specific miRNA changes in the heart and brain [22]. That study has reported that, in the heart, miR-1 of SIDS infants was down-regulated compared with controls [22]. Among the diverse array of miRNAs, miR-1 is a key regulator of cardiac electrical remodeling systems, such as ion channel expression [23]. miR-1 functions as a negative regulator of connexin 43 (Cx43), a major gap junction protein, and Kir2.1 [24], an inward-rectifier potassium channel, in cardiomyocytes [25]. Dysregulation of cardiac-abundant miR-1 has been shown to be injurious to cardiomyocytes and the heart. miR-1 leaks from injured cardiomyocytes in a form packed in EVs or in a protein-bound state [26]. A previous study identified plasma EV miR-208b-3p as a promising biomarker for predicting sudden cardiac death in acute coronary syndrome (ACS) patients and potentially useful for postmortem forensic diagnosis of death due to ACS [27]. Furthermore, the plasma concentration of miR-208b-3p, a myo-miR, reportedly increases significantly within 1 h in rats with coronary artery occlusion [28]. As EV-packed miR-208 is rapidly released into the blood from the heart in response to cardiac damage, it may be useful as a SIDS marker, similar to miR-1.

Furthermore, EV myo-miRs down-regulate CXC chemokine receptor 4 (CXCR4) in bone marrow mononuclear cells [18]. CXCR4 negatively regulates β-adrenergic receptor (β-AR) signaling and ultimately limits β-adrenergic diastolic Ca^{2+} accumulation in cardiac myocytes [29]. The KEGG pathway analysis showed that expression of the α-AR gene is decreased in cardiomyocytes of SIDS infants (Fig. 4F). Although expression of the β-AR did not change in

SIDS, expression of its downstream G-protein subunits, such as Gαs and Gαi, was reduced. Imbalances in β-AR and muscarinic acetylcholine receptor (mAChR) expression have been linked to SIDS [30]. The results of the present study suggest that CXCR4 down-regulation by myo-miRs increases β-AR expression, which leads to an imbalance in β-AR and mAChR expression that in turn affects the pathogenesis of SIDS.

The comparison of serum-derived EV miRNA expression showed that 38 miRNAs are significantly down-regulated in SIDS. Among them, miR-122 levels have been reported to be decreased in plasma and increased in the infarct area in patients with myocardial infarction [31]. Down-regulation of serum-derived EV miR-122 may be involved in SIDS pathogenesis.

The significant enrichment of GO annotations and their interconnections was dominated by protein phosphorylation, the actin cytoskeleton and myosin complex, and kinase activity (Fig. 4A, 4B). KEGG analysis indicated that genes related to cardiac muscle contraction pathways are markedly down-regulated in SIDS (Fig. 5B). Myofilament activation and contractility are governed by the thin actin and thick myosin filament proteins. Defects in the response of myofilaments to Ca^{2+} may be related to cardiac dysfunction [32]. These results suggest that abnormalities in myofilaments caused by dysregulation of the actin cytoskeleton and myosin complex contribute to cardiac dysfunction in SIDS.

Calcium signaling is an essential regulatory mechanism for cardiac contraction and electrical signaling in the heart, governing heart rhythm and controlling cardiac cell growth [33,34]. To ensure heart health, Ca^{2+} signals must be tightly controlled, and impairments in Ca^{2+} handling proteins generally lead to progressive heart failure or sudden cardiac death. The KEGG analysis of the present study indicated that NCX genes are down-regulated in SIDS (Fig. 5B, 5C). NCX1 has been identified as one of the most important proteins involved in controlling the distribution of intracellular Ca^{2+} [35]. NCX1-dependent inactivation plays an essential role in

heart function by affecting both cardiac excitability and contractility.

We found that Ca^{2+} signaling pathways are involved in the marked down-regulation of genes associated with Ca^{2+} channels in SIDS (Fig. 5C). Calcium-release units of the junctional sarcoplasmic reticulum (SR) are formed by stable uniform complexes consisting of four proteins: ryanodine receptor (RyR), calsequestrin, triadin (TRDN), and JCN [36]. These four proteins are required for normal Ca^{2+} release via the SR Ca^{2+}-release channel. KEGG analysis shows that expression of the JCN and TRDN genes is decreased in SIDS. Knockout of TRDN reportedly leads to the loss of cardiac Ca^{2+}-release units, impaired excitation-contraction coupling, and cardiac arrhythmias in mice and isolated myocytes [37]. In addition, JCN plays prominent roles in the Ca^{2+} cycle and contractility of cardiomyocytes [38]. Molecular interactions between DHPR, a voltage-dependent Ca^{2+}-channel gate, and RyR are essential in the process of excitation-contraction coupling in the heart. SERCA2a also plays a central role in contraction and relaxation of the heart [33]. Postmortem genetic analyses indicated that mutations in RyR2 are associated with SIDS [39]. Dysregulation of SERCA2a is a hallmark of heart disease [40,41]. Taken together, these data suggest that down-regulation of genes associated with Ca^{2+} signaling contributes to the pathophysiology of SIDS.

KEGG analyses indicated that the MAPK and Ras signaling pathways are significantly associated with SIDS (Fig. 5A). Figure 5E shows that a number of genes related to the MAPK pathway are markedly down-regulated in SIDS. The MAPK pathway plays a variety of roles in humans [42]. Cardiac myocytes can respond to changes in hemodynamics by activating multiple intracellular signaling pathways that have been implicated in the maintenance and regulation of myocardial function. Mechanical loading can be sensed by cardiomyocytes via a diverse group of membrane-anchored mechanosensors such as ion channels, growth-factor receptors, and integrins. MAPK family underscored by the activation of Ras, and Janus-activated protein

kinase (JAK)/signal transducer and activator of transcription (STAT) pathway are involved in these cardiac functions. Changes in the mechanical transmission of signaling stimuli can result in disease conditions [42]. In SIDS, various genes associated with these pathways are down-regulated, suggesting that the MAPK and JAK/STAT signaling pathways may be involved in the pathogenesis of the disease.

Previous studies have reported that cardiac injury, such as dysregulation of cardiac conduction or cardiomyopathy, could potentially contribute to the risk of SIDS [43,44]. Hyperthermia and heart stress are common findings in SIDS infants, and heat stress can act in concert with other environmental factors, such as exposure to cigarette smoke [45]. Although the number of reports is limited, an association between SIDS risk and heart disease has also been examined, primarily in terms of mutations in heart-related genes [46]. Regarding miRNAs associated with SIDS, specific up-regulation of miR-1 and let-7b in the heart and brain, respectively, has been reported [22].

One limitation of the present study is that quantitative measurements of EV miRNAs was not performed due to the small amount of serum obtained from SIDS cases. Further studies with accumulated cases will be required to improve early detection, establish diagnostic markers for SIDS, and elucidate the associated pathological changes. The results of this study, however, suggest that EV miRNAs are potentially useful as markers for determining the cause of death.

In conclusion, serum-derived EV miRNAs have enormous potential for revealing the pathophysiological changes associated with SIDS. In serum-derived EVs from SIDS cases, significant up-regulation of myocardial-specific miRNAs, such as miR-1, -208, and -499, was detected. The increased expression of miR-1, -208, and -499 in serum-derived EVs suggests these may be the most promising candidate markers. Furthermore, GO and KEGG enrichment analyses indicated that the expression of genes contributing to cardiac ion channels in SIDS is

significantly reduced. Collectively, these findings suggest that the pathogenesis of SIDS may be associated with cardiac injury.

MATERIALS AND METHODS

Chemicals

The chemicals and reagents used in this study were as follows: anti-CD9 antibody (#sc-59140), anti-CD63 (#sc-5275) antibody, radioimmunoprecipitation (RIPA) buffer containing a protease inhibitor, phenylmethylsulfonyl fluoride, and sodium orthovanadate were obtained from Santa Cruz Biotechnology (#SC-24948, Santa Cruz, CA). Polyvinylidene difluoride (PVDF) Blocking Reagent was obtained from TOYOBO (#NYPBR01, Osaka, Japan); ECL™ prime western detection reagent was obtained from Cytiva (#RPN2232, Marlborough, MA); and horseradish peroxidase (HRP)-tagged anti-mouse immunoglobulin G (IgG) was obtained from MBL (#330, Nagoya, Japan). Halt™ phosphatase inhibitor cocktail (#78420) and bicinchoninic acid protein assay kit (#A65453) were obtained from Thermo Fisher Scientific (Waltham, MA), and the miRNeasy micro kit was obtained from Qiagen (#217084, Hilden, Germany).

Autopsy cases

All cases were autopsied between 2018 and 2024 at the Department of Forensic Medicine, Nagoya City University Graduate School of Medical Sciences. Table 1 summarizes the case profiles. A total of 8 cases, 4 each of SIDS and CT, were selected for EV miRNA analysis. As described earlier, infants who died from known causes were classified as CT. The cadavers were preserved for 6-9 h at room temperature (below 25°C) and then stored at 4°C.

Serum collection from autopsy cases and exosome isolation

Blood samples were collected without anti-coagulant from 8 cadavers at autopsy and centrifuged at 1,500 *g* for 10 min at 4°C. After centrifugation, the resulting serum was stored at −80°C until use. EV extraction was performed using an ultracentrifugation method. Briefly, an aliquot (0.5 mL) of serum was diluted with 9.5 mL of phosphate-buffered saline (PBS) and centrifuged at 10,000 *g* for 20 min at 4°C to remove debris, followed by filtration through a 0.45-μm pore filter (Millex-HV Filter Unit, #SLHV004SL, Merck Millipore, Darmstadt, Germany). The filtered serum was ultracentrifuged at 100,000 *g* for 70 min at 4°C (Optime TLX, Beckman Coulter, Krefeld, Germany). Pelleted EVs were washed with PBS and then ultracentrifuged at 100,000 *g* for 70 min at 4°C. After resuspension of pelleted EVs in PBS, the resulting EV fraction was used for RNA isolation and EV characterization. The presence of EVs was confirmed by morphological observation using SEM. The EVs were lysed using RIPA buffer, and the levels of CD9 and CD63 proteins were determined using western blotting. Size distribution was analyzed using DLS with a Zeta-potential & Particle Size Analyzer (Malvern Panalytical, Malvern, UK).

miRNA extraction and sample quality control

EV miRNAs in serum were extracted using a miRNeasy micro kit in accordance with the manufacturer's instructions. After miRNA extraction, the RNA was eluted in RNase-free water. Analyses of all cadavers were performed using the same amount of RNA. The integrity and quality of enriched EV miRNA samples were assessed using Nanodrop One (Thermo Fisher Scientific, Waltham, MA). The yield and distribution of small RNA were determined using an Agilent 2100 Bioanalyzer with an RNA Nano 6000 Assay kit (#5067-1511, Agilent Technologies, Santa Clara, CA).

Library construction, quality control, and sequencing

A total amount of 10 ng of RNA per sample was used as input material for the small RNA library. Sequencing libraries were generated using a Small RNA Lib Prep kit for Illumina V3 (#RK20302, Abclonal Technology, Woburn, MA) following the manufacturer's recommendations. All adapters were diluted 5-fold to achieve the appropriate concentration for EV RNAs. The incubation time for 3'-adapter ligation was extended to 3 h at 30°C to enhance connection efficiency. PCR products were purified on an 8% polyacrylamide gel (100 V, 80 min). Libraries containing insertion fragments of 18-40 bp were selected, and quality was assessed on the Agilent 2100 Bioanalyzer using DNA High Sensitivity Chips (Agilent Technologies). The libraries were pooled and sequenced on a NovaSeq 6000 (Illumina, San Diego, CA) using a NovaSeq 6000 S4 Reagent kit, v1.5 (100 cycles), (#20028316, Illumina) in SE50 mode.

Data analysis

Low-quality reads or reads with adapters and poly-N tails were discarded using fastp [47] for quality control. After quality control, the reads are mapped to the genome (Ensembl 112 *Homo sapiens* GRCh38 primary) using Bowtie [48]. The mapped reads were annotated against miRBase. To ensure that each unique small RNA was assigned to a single category, a priority order was followed: known miRNA > rRNA > tRNA > snRNA > snoRNA > repeat > gene > novel miRNA. Reads annotated as known miRNAs were analyzed using by miRDeep2 [49] and SRna-Tools-CLI. Novel miRNAs were predicted from the remaining unannotated reads based on their hairpin structure using miREvo [50] and miRDeep2.

The expression of known and unique miRNAs in each sample was statistically analyzed and normalized by transcript per kilobase million (e.g., [read count * 1,000,000]/[total miRNA read

count]) [51]. A family analysis was then performed on the detected miRNAs. Known miRNAs were assigned to families using miFam.dat from miRBase, whereas novel miRNAs were classified by searching against the RFam database. Subsequently, DESeq2 (version 1.28.0) [52] was used to perform differential expression analysis between comparison groups, with a significance threshold of $p \leq 0.05$ and $|\log2FoldChange| \geq 1$. To understand the biological functions of the differentially expressed miRNAs, their target genes were predicted using R package edgeR (version 3.24.3) and RNAhybrid [53], and the intersection of the results was used. Finally, GO and KEGG pathway enrichment analyses were performed on the predicted target genes using clusterProfiler [54], with a significance threshold of adjusted p-value < 0.05.

Ethical approval

This study was approved by the Institutional Review Board for the Protection of Human Subjects in Research at Nagoya City University (approval number: 60-24-0135, approval date: Jan. 25, 2022). All the procedures were approved and performed in accordance with the ethical standards laid down in the 1964 Declaration of Helsinki. This study was conducted based on the "Ethical Guidelines for Medical Research Involving Human Subjects (enacted by the Ministry of Health, Labor, and Welfare in Japan)." Information on the implementation of the study was posted on clinical Research Management Center, Nagoya City University Hospital website (https://ncu-cr.jp/patient/clinical_research/clinical_research_cont-2). If bereaved family requested to refuse not be used for research purposes, they were excluded from the study.

DECLARATIONS

Acknowledgements

This work was supported by a Grant-in-Aid for Research from Nagoya City University (grant number 2412004). We acknowledge the assistance of the Research Equipment Sharing Center at Nagoya City University. This work was the result of using research equipment shared with the MEXT Project for Promoting Public Utilization of Advanced Research Infrastructure (Program for Supporting Construction of Core Facilities), grant number JPMXS0441500025. We would also like to thank Dr. Hiroshi Takase of the Research Equipment Sharing Center of Nagoya City University for assistance with scanning electron microscopy observations.

Author contributions

SK: conceived and designed the experiments. SK, MF, JM, YN: performed the experiments and analyzed the data. MF, HK, TO: performed the autopsies and examinations. SK, MF: wrote the manuscript with contributions from co-authors. TO: project administration.

Conflicts of interest

The authors declare that they have no conflicts of interest.

Data Availability

The data have been deposited with links to BioProject accession number PRJDB37850 in the DDBJ BioProject database.

References

1 Baruteau, A.-E., Tester, D. J., Kapplinger, J. D., Ackerman, M. J. & Behr, E. R. Sudden infant death syndrome and inherited cardiac conditions. *Nat. Rev. Cardiol.* **14**, 715-726, https://doi.prg/10.1038/nrcardio.2017.129 (2017).

2 Harrington, C. T., Hafid, N. A. & Waters, K. A. Butyrylcholinesterase is a potential biomarker for Sudden Infant Death Syndrome. *EBioMedicine* **80**, 104041, https://doi.org/10.1016/j.ebiom.2022.104041 (2022).

3 Ferrante, L., Opdal, S. H. & Byard, R. W. Further exploration of the influence of immune proteins in Sudden Infant Death Syndrome (SIDS). *Acta Paediatrica*, https://doi.org/10.1111/apa.70197 (2025).

4 Graham, S. F., Chevallier, O. P., Kumar, P., Türkoğlu, O. & Bahado-Singh, R. O. Metabolomic profiling of brain from infants who died from Sudden Infant Death Syndrome reveals novel predictive biomarkers. *J. Perinatol.* **37**, 91-97, https://doi.org/10.1038/jp.2016.139 (2017).

5 Goldstein, R. D. et al. Inconsistent classification of unexplained sudden deaths in infants and children hinders surveillance, prevention and research: recommendations from The 3rd International Congress on Sudden Infant and Child Death. *Forensic Sci. Med. Path.* **15**, 622-628, https://doi.org/10.1007/s12024-019-00156-9 (2019).

6 Filiano, J. J. & Kinney, H. C. A perspective on neuropathologic findings in victims of the sudden infant death syndrome: the triple-risk model. *Biol. Neonate* **65**, 194-197, http://doi.org/10.1159/000244052 (1994).

7 Horne, R. S. C., Harrewijn, I. & Hunt, C. E. Physiology during sleep in preterm infants: Implications for increased risk for the sudden infant death syndrome. *Sleep Med. Rev.* **78**, 101990, https://doi.org/10.1016/j.smrv.2024.101990 (2024).

8 Neubauer, J. et al. Post-mortem whole-exome analysis in a large sudden infant death syndrome cohort with a focus on cardiovascular and metabolic genetic diseases. *Eur. J. Hum. Genet.* **25**, 404-409, https://doi.org/10.1038/ejhg.2016.199 (2017).

9 Van Norstrand, D. W. & Ackerman, M. J. Genomic risk factors in sudden infant death syndrome. *Genome Med.* **2**, 86, https://doi.org/10.1186/gm207 (2010).

10 Hessvik, N. P. & Llorente, A. Current knowledge on exosome biogenesis and release. *Cell. Mol. Life Sci.* **75**, 193-208, https://doi.org/10.1007/s00018-017-2595-9 (2018).

11 Liu, T. et al. EVmiRNA: a database of miRNA profiling in extracellular vesicles. *Nucleic Acids Res.* **47**, D89-D93, https://doi.org/10.1093/nar/gky985 (2019).

12 Ambros, V. The functions of animal microRNAs. *Nature* **431**, 350-355,

https://doi.org/10.1038/nature02871 (2004).

13 Mori, M. A., Ludwig, R. G., Garcia-Martin, R., Brandao, B. B. & Kahn, C. R. Extracellular miRNAs: From biomarkers to mediators of physiology and disease. *Cell Metab.* **30**, 656-673, https://doi.org/10.1016/j.cmet.2019.07.011 (2019).

14 Dash, B. P. et al. Upregulated miR-10b-5p as a potential miRNA signature in amyotrophic lateral sclerosis patients. *Front. Cell Neurosci.* **18**, 1457704, https://doi.org/10.3389/fncel.2024.1457704 (2024).

15 Kanno, S., Sakamoto, T., Fukuta, M., Kato, H. & Aoki, Y. Stability of exosomes in the postmortem serum and preliminary study on exosomal miRNA expression profiling in serum from myocardial infarction cadavers. *Int. J. Legal Med.* **137**, 825-834, https://doi.org/10.1007/s00414-022-02913-y (2023).

16 Kanehisa, M., Furumichi, M., Sato, Y., Matsuura, Y. & Ishiguro-Watanabe, M. KEGG: biological systems database as a model of the real world. *Nucleic Acids Res.* **53**, D672-d677, http://doi.org/10.1093/nar/gkae909 (2025).

17 Deddens, J. C. et al. Circulating extracellular vesicles contain miRNAs and are released as early biomarkers for cardiac injury. *J. Cardiovasc. Transl. Res.* **9**, 291-301, https://doi.org/10.1007/s12265-016-9705-1 (2016).

18 Cheng, M. et al. Circulating myocardial microRNAs from infarcted hearts are carried in exosomes and mobilise bone marrow progenitor cells. *Nat. Commun.* **10**, 959, https://doi.org/10.1038/s41467-019-08895-7 (2019).

19 Chistiakov, D. A., Orekhov, A. N. & Bobryshev, Y. V. Cardiac extracellular vesicles in normal and infarcted heart. *Int. J. Mol. Sci.* **17** (2016).

20 Crouser, E. D. et al. Circulating exosomal microRNA expression patterns distinguish cardiac sarcoidosis from myocardial ischemia. *PLoS One* **16**, e0246083, https://doi.org/10.1371/journal.pone.0246083 (2021).

21 Zhang, L. et al. Circulating miR-499 are novel and sensitive biomarker of acute myocardial infarction. *J. Thorac. Dis.* **7**, 303-308, https://doi.org/10.3978/j.issn.2072-1439.2015.02.05 (2015).

22 Courts, C., Grabmüller, M. & Madea, B. Dysregulation of heart and brain specific micro-RNA in sudden infant death syndrome. *Forensic Sci. Int.* **228**, 70-74, https://doi.org/10.1016/j.forsciint.2013.02.032 (2013).

23 Yang, B. et al. The muscle-specific microRNA miR-1 regulates cardiac arrhythmogenic potential by targeting GJA1 and KCNJ2. *Nat. Med.* **13**, 486-491, https://doi.org/10.1038/nm1569 (2007).

24 Yang, D. et al. MicroRNA-1 deficiency is a primary etiological factor disrupting cardiac contractility and electrophysiological homeostasis. *Circ. Arrhythm.*

Electrophysiol. **17**, e012150, https://doi.org/10.1161/CIRCEP.123.012150 (2024).

25 Xu, H. F. et al. MicroRNA- 1 represses Cx43 expression in viral myocarditis. *Mol. Cell Biochem.* **362**, 141-148, https://doi.org/10.1007/s11010-011-1136-3 (2012).

26 Liu, X. et al. Plasma miR-1, miR-208, miR-499 as potential predictive biomarkers for acute myocardial infarction: An independent study of Han population. *Exp. Gerontol.* **72**, 230-238, https://doi.org/10.1016/j.exger.2015.10.011 (2015).

27 Huang, S. et al. Plasma extracellular vesicles microRNA-208b-3p and microRNA-143-3p as novel biomarkers for sudden cardiac death prediction in acute coronary syndrome. *Mol. Omics* **19**, 262-273, https://doi.org/10.1039/d2mo00257d (2023).

28 Zhao, X., Wang, Y. & Sun, X. The functions of microRNA-208 in the heart. *DRCP* **160**, 108004, https://doi.org/10.1016/j.diabres.2020.108004 (2020).

29 LaRocca, T. J. et al. CXCR4 cardiac specific knockout mice develop a progressive cardiomyopathy. *Int. J. Mol. Sci.* **20**, https://doi.org/10.3390/ijms20092267 (2019).

30 Garofolo, M. C., Seidler, F. J., Auman, J. T. & Slotkin, T. A. beta-Adrenergic modulation of muscarinic cholinergic receptor expression and function in developing heart. *Am. J. Physiol. Regul. Integr. Comp. Physiol.* **282**, R1356-1363, https://doi.org/10.1152/ajpregu.00598.2001 (2002).

31 D'Alessandra, Y. et al. Circulating microRNAs are new and sensitive biomarkers of myocardial infarction. *Eur. Heart J.* **31**, 2765-2773, https://doi.org/10.1093/eurheartj/ehq167 (2010).

32 Sequeira, V., Nijenkamp, L. L. A. M., Regan, J. A. & van der Velden, J. The physiological role of cardiac cytoskeleton and its alterations in heart failure. *BBA Biomembranes* **1838**, 700-722, https://doi.org/10.1016/j.bbamem.2013.07.011 (2014).

33 Bers, D. M. Cardiac excitation-contraction coupling. *Nature* **415**, 198-205, https://doi.org/10.1038/415198a (2002).

34 Olesen, C. et al. The structural basis of calcium transport by the calcium pump. *Nature* **450**, 1036-1042, https://doi.org/10.1038/nature06418 (2007).

35 Scranton, K. et al. Cardiac function is regulated by the sodium-dependent inhibition of the sodium-calcium exchanger NCX1. *Nat. Commun.* **15**, 3831, https://doi.org/10.1038/s41467-024-47850-z (2024).

36 Zhang, L., Kelley, J., Schmeisser, G., Kobayashi, Y. M. & Jones, L. R. Complex formation between junctin, triadin, calsequestrin, and the ryanodine receptor: Proteins of the cardiac junctional sarcoplasmic reticulum membrane. *J. Biol. Chem.*

272, 23389-23397, https://doi.org/10.1074/jbc.272.37.23389 (1997).

37 Chopra, N. et al. Ablation of triadin causes loss of cardiac Ca2+ release units, impaired excitation-contraction coupling, and cardiac arrhythmias. *Proc. Natl. Acad. Sci. U S A* **106**, 7636-7641, https://doi.org/10.1073/pnas.0902919106 (2009).

38 Fan, G.-C., Yuan, Q., Zhao, W., Chu, G. & Kranias, E. G. Junctin is a prominent regulator of contractility in cardiomyocytes. *Biochem. Biophys. Res. Commun.* **352**, 617-622, https://doi.org/10.1016/j.bbrc.2006.11.093 (2007).

39 Son, M. J., Kim, M. K. & Yoo, S. H. Identification of mutations of the RYR2 in Sudden Infant Death Syndrome. *J. Korean Med. Sci.* **40**, e17, https://doi.org/10.3346/jkms.2025.40.e17 (2025).

40 Shooshtarian, A. K., O'Gallagher, K., Shah, A. M. & Zhang, M. SERCA2a dysfunction in the pathophysiology of heart failure with preserved ejection fraction: a direct role is yet to be established. *Heart Fail. Rev.* **30**, 545-564, https://doi.org/10.1007/s10741-025-10487-1 (2025).

41 Park, J. H. & Kho, C. MicroRNAs and calcium signaling in heart disease. *Int. J. Mol. Sci.* **22**, https://doi.org/10.3390/ijms221910582 (2021).

42 Jaalouk, D. E. & Lammerding, J. Mechanotransduction gone awry. *Nat. Rev. Mo. l Cell Biol.* **10**, 63-73, https://doi.org/10.1038/nrm2597 (2009).

43 Ottaviani, G., Leonardi, P., Del Fabbro, M. & Ramos, S. G. Sudden unexpected infant and perinatal death: pathological findings of the cardiac conduction system. *Diagnostics* **15** (2025).

44 Dettmeyer, R. B. & Kandolf, R. Cardiomyopathies--misdiagnosed as Sudden Infant Death Syndrome (SIDS). *Forensic Sci. Int.* **194**, e21-24, https://doi.org/10.1016/j.forsciint.2009.10.010 (2010).

45 Bach, V. & Libert, J. P. Hyperthermia and heat stress as risk factors for sudden infant death syndrome: A narrative review. *Front Pediatr.* **10**, 816136, https://doi.org/10.3389/fped.2022.816136 (2022).

46 Köffer, J., Scheiper-Welling, S., Verhoff, M. A., Bajanowski, T. & Kauferstein, S. Post-mortem genetic investigation of cardiac disease-associated genes in sudden infant death syndrome (SIDS) cases. *Int. J. Legal Med.* **135**, 207-212, https://doi.org/10.1007/s00414-020-02394-x (2021).

47 Chen, S., Zhou, Y., Chen, Y. & Gu, J. fastp: an ultra-fast all-in-one FASTQ preprocessor. *Bioinformatics* **34**, i884-i890, https://doi.org/10.1093/bioinformatics/bty560 (2018).

48 Langmead, B., Trapnell, C., Pop, M. & Salzberg, S. L. Ultrafast and memory-efficient alignment of short DNA sequences to the human genome. *Genome Biol.*

10, R25, https://doi.org/10.1186/gb-2009-10-3-r25 (2009).

49 Friedländer, M. R., Mackowiak, S. D., Li, N., Chen, W. & Rajewsky, N. miRDeep2 accurately identifies known and hundreds of novel microRNA genes in seven animal clades. *Nucleic Acids Res.* **40**, 37-52, https://doi.org/10.1093/nar/gkr688 (2012).

50 Wen, M., Shen, Y., Shi, S. & Tang, T. miREvo: an integrative microRNA evolutionary analysis platform for next-generation sequencing experiments. *BMC Bioinformatics* **13**, 140, https://doi.org/10.1186/1471-2105-13-140 (2012).

51 Zhou, L. et al. Integrated profiling of microRNAs and mRNAs: microRNAs located on Xq27.3 associate with clear cell renal cell carcinoma. *PLoS One* **5**, e15224, https://doi.org/10.1371/journal.pone.0015224 (2010).

52 Love, M. I., Huber, W. & Anders, S. Moderated estimation of fold change and dispersion for RNA-seq data with DESeq2. *Genome Biol.* **15**, 550, https://doi.org/10.1186/s13059-014-0550-8 (2014).

53 Kruger, J. & Rehmsmeier, M. RNAhybrid: microRNA target prediction easy, fast and flexible. *Nucleic Acids Res.* **34**, W451-454, https://doi.org/10.1093/nar/gkl243 (2006).

54 Yu, G., Wang, L. G., Han, Y. & He, Q. Y. clusterProfiler: an R package for comparing biological themes among gene clusters. *Omics* **16**, 284-287, https://doi.org/10.1089/omi.2011.0118 (2012).

Figure Legends

Fig. 1. Characterization of serum-derived EVs by size distribution (A), morphology (B), and western blot analyses of CD9 and CD63 levels (C).

Isolated EVs were suspended in 100 μL of PBS. (A) Measurement of EV size using DLS. (B) SEM observation of EV morphology. Scale bar=200 nm. Figure shows a typical example. (C) The lysate of the resulting EV fraction was resolved by SDS-PAGE and electroblotted onto a PVDF membrane. The blot was probed with anti-CD9 and -CD63 antibodies, followed by a corresponding HRP-tagged secondary antibody.

Fig. 2. Quality control of small RNAs derived from serum of SIDS and CT infants.

Electropherograms generated by Bioanalyzer showing peak distribution and fluorescence intensity. Small RNAs were extracted from serum-derived EVs of SIDS (lower panel) and CT (upper panel) infants; x-axis: size in bases, y axis: fluorescence intensity.

Fig. 3. Differentially expressed serum-derived EV miRNAs between SIDS and CT.

(A) Venn diagram of differentially expressed miRNAs. (B) Volcano plot generated based on miRNA expression profile. Red and green indicate significant up- or down-regulation of miRNA expression >2-fold in EVs from SIDS compared with those from CT. (C) Clustering heat map of differentially expressed miRNAs in SIDS (right 4 columns) and CT (left 4 columns). The intensity $\log_2$ plot indicates relatively higher (red) and lower (blue) expression.

Fig. 4. GO analyses of EV miRNA-targeted genes.

GO enrichment and KEGG pathways analyses of predicted miRNA target genes. (A) GO enrichment results showing differences in target genes based on distribution according to GO

terms. BP: Biological Process, CC: Cellular Component, MF: Molecular Function. (B) The y-axis represents pathway enrichment, and the x-axis represents gene ratio. The gene ratio indicates the percentage of GO term annotated genes in SIDS and CT.

Fig. 5. KEGG pathway analysis of EV miRNA-targeted genes.

(A) KEGG pathway enrichment scatter plot of differential expressed genes between SIDS and CT. (B) Cardiac muscle contraction cascade pathway identified by KEGG analysis. (C) Calcium signaling pathway. (D) Adrenergic signaling in cardiomyocytes. (E) MAPK signaling pathway. (F) Regulation of actin cytoskeleton. (B)-(F) Genes are colored according to Gene Set Enrichment Analysis calculated scores for SIDS versus CT; the most vivid green and red genes belong to the core enrichment.

Table 1 Characteristics of cases examined in this study

Cases	Age Male/Female	Cause of death	Medical history	Drug test	PMI (Morgue) hr	Sampling (blood from heart)
CT-1	5 m M	Dehydration		N.T.	10 (2)	Left
CT-2	1 y 5 m M	Airway Obstruction		N.T.	19 (13)	Right
CT-3	4 m M	Invagination		N.T.	26 (19)	Right
CT-4	5 m F	Aspiration Pneumonia	Charge Syndrome	(-) Triage	13 (6)	Right
SIDS-1	4 m F	SIDS		N.T.	22 (13)	Right
SIDS-2	3 m F	SIDS		N.T.	24 (17)	Right
SIDS-3	6 m M	SIDS		(-) IVeX	20 (11)	Left
SIDS-4	3 m M	SIDS		N.T.	25 (19)	Right

Age, y : year, m : month, M : Male, F : Female, PMI : postmortem interval, including storage

interval in morgue. N.T. : not tested. Triage and IVeX: drug screening kit

Table 2 Number of the mapped reads obtained from miRNA sequencing of the SIDS and control (CT) groups

Group of Reads	Number of Reads							
	CT-1	CT-2	CT-3	CT-4	SIDS-1	SIDS-2	SIDS-3	SIDS-4
Raw reads	10847569	12030582	14136955	11418606	13349069	11065120	11913171	11956368
Clean reads	10670884	11812701	13976212	11229412	12989172	9563826	11722110	11782478
Clean reads (%)	98.37%	98.19%	98.86%	98.34%	97.30%	86.43%	98.40%	98.55%
small RNA reads	10543274	11694773	13925248	11156062	12860834	9146570	11643078	11597573

Table 3 Significantly up- and down-regulated miRNAs of serum-derived EVs in cadavers SIDS versus CT infants

Up-regulated miRNA	SIDS readcount	CT readcount	Fold change (log2)	p-value	padj
hsa-miR-208b-3p	11.241	1.346	2.876	0.030	0.617
hsa-miR-659-5p	11.250	1.725	2.825	0.026	0.611

hsa-miR-493-5p	55.739	9.079	2.614	0.010	0.498
hsa-miR-27a-5p	89.194	16.797	2.413	0.010	0.498
hsa-miR-1246	397.684	89.308	2.155	0.009	0.498
hsa-miR-483-3p	98.385	23.637	2.028	0.019	0.537
hsa-miR-218-5p	130.830	37.290	1.798	0.004	0.462
hsa-miR-128-3p	550.162	179.676	1.611	0.003	0.356
hsa-miR-499b-3p	664.673	221.083	1.586	0.019	0.537
hsa-miR-499a-5p	666.440	222.118	1.583	0.019	0.537
hsa-miR-10b-5p	1315.185	448.646	1.551	0.028	0.617
hsa-miR-23b-3p	99.714	37.054	1.431	0.034	0.663
hsa-miR-335-3p	38.236	14.598	1.395	0.046	0.747
hsa-miR-1-3p	1602.540	701.612	1.192	0.012	0.515

Down-regulated miRNA	SIDS readcount	CT readcount	Fold change (log2)	p-value	padj
hsa-miR-4686	0.000	6.298	-5.342	0.002	0.269
hsa-miR-192-3p	0.476	6.625	-3.761	0.021	0.537
hsa-miR-193b-5p	1.154	16.753	-3.730	0.001	0.191
hsa-miR-21-3p	1.850	21.796	-3.540	0.000	0.103
hsa-miR-194-3p	0.799	5.889	-3.045	0.044	0.747
hsa-miR-107	31.186	248.329	-2.996	0.000	0.103
hsa-miR-455-3p	4.437	30.696	-2.742	0.001	0.224
hsa-let-7g-3p	1.719	10.297	-2.603	0.037	0.680
hsa-miR-1299	4.228	23.678	-2.447	0.043	0.747
hsa-miR-885-3p	7.620	38.486	-2.349	0.007	0.472
hsa-miR-548am-3p	3.948	18.484	-2.211	0.017	0.537
hsa-miR-203a-3p	8.011	31.190	-1.975	0.007	0.472
hsa-miR-203b-5p	8.011	31.190	-1.975	0.007	0.472
hsa-miR-660-5p	6.818	23.933	-1.861	0.037	0.680
hsa-miR-675-3p	17.443	62.924	-1.859	0.044	0.747
hsa-miR-184	11.800	41.001	-1.829	0.031	0.617
hsa-miR-29b-3p	12.838	43.596	-1.745	0.024	0.596
hsa-miR-22-3p	463.222	1545.715	-1.739	0.001	0.224
hsa-miR-548aq-3p	8.875	28.886	-1.739	0.015	0.537
hsa-miR-548g-5p	8.875	28.886	-1.739	0.015	0.537

hsa-miR-19b-3p	9.332	29.532	-1.652	0.041	0.744
hsa-miR-199b-5p	41.874	118.195	-1.502	0.011	0.515
hsa-miR-103b	156.336	421.214	-1.432	0.007	0.472
hsa-miR-29a-3p	336.376	898.822	-1.419	0.019	0.537
hsa-miR-103a-3p	158.933	423.557	-1.416	0.007	0.472
hsa-miR-148a-3p	1025378.131	2701952.274	-1.398	0.012	0.515
hsa-miR-192-5p	8049.115	20885.406	-1.376	0.009	0.498
hsa-miR-320c	38.034	95.895	-1.333	0.027	0.617
hsa-miR-885-5p	236.997	582.260	-1.297	0.019	0.537
hsa-miR-148b-3p	911.733	2172.736	-1.253	0.013	0.515
hsa-miR-502-3p	28.199	67.054	-1.238	0.032	0.631
hsa-miR-30e-5p	445.308	1046.445	-1.233	0.019	0.537
hsa-miR-152-3p	127.268	288.367	-1.182	0.029	0.617
hsa-miR-194-5p	685.462	1551.403	-1.179	0.031	0.617
hsa-miR-122b-3p	1076488.887	2201700.294	-1.032	0.021	0.537
hsa-miR-122-5p	1076528.719	2201732.087	-1.032	0.021	0.537

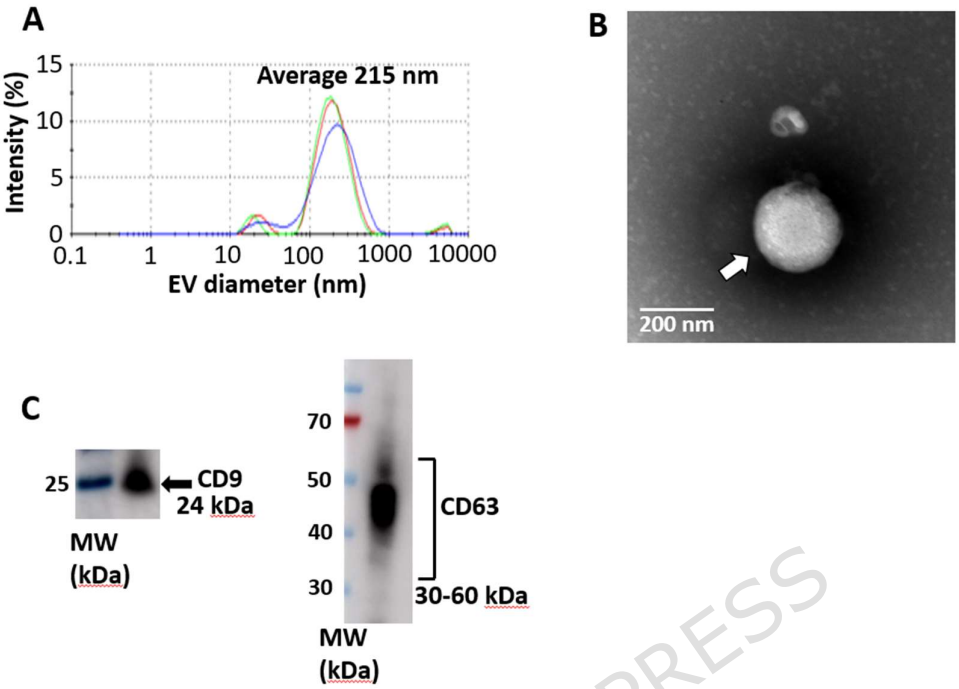

Fig. 1

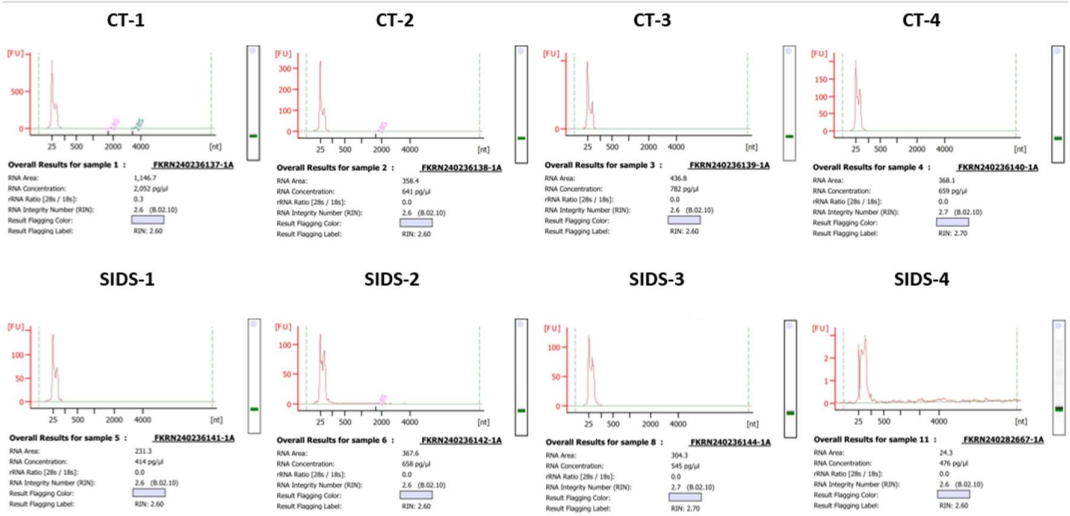

Fig. 2

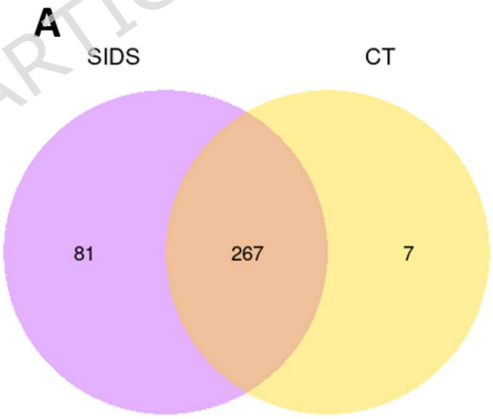

Fig. 3

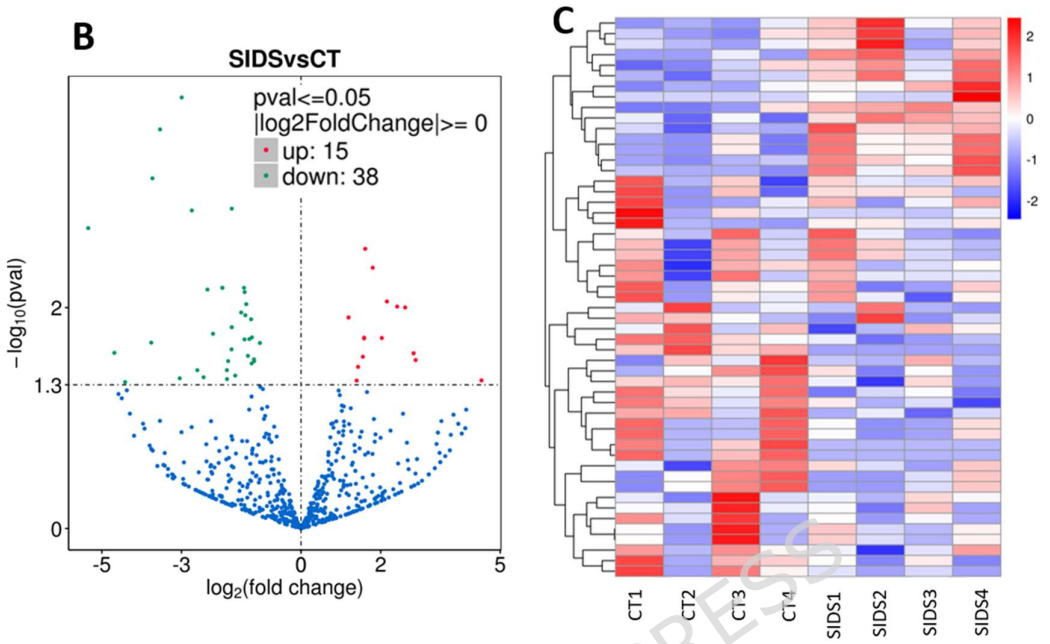

Fig. 3

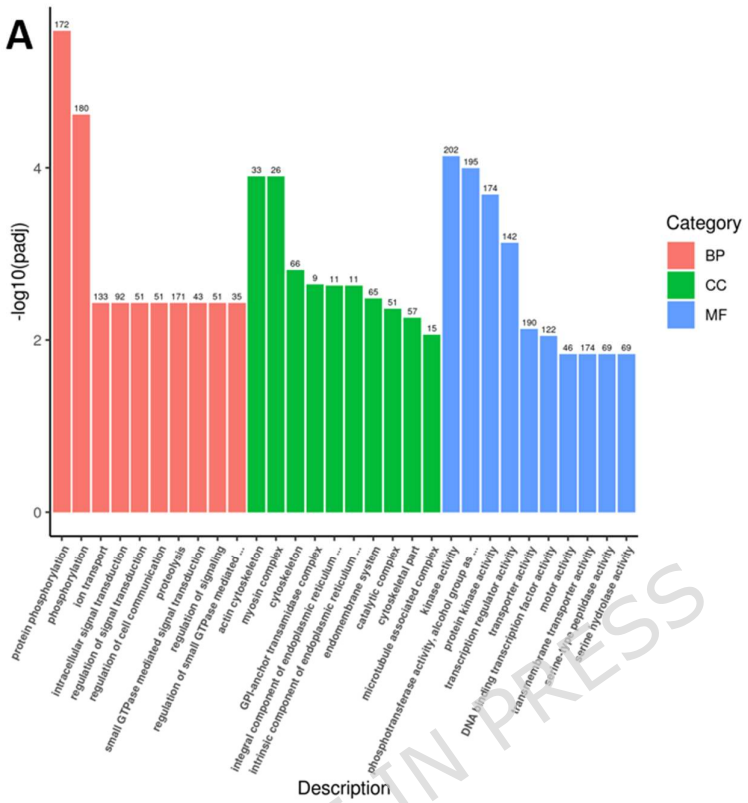

Fig. 4A

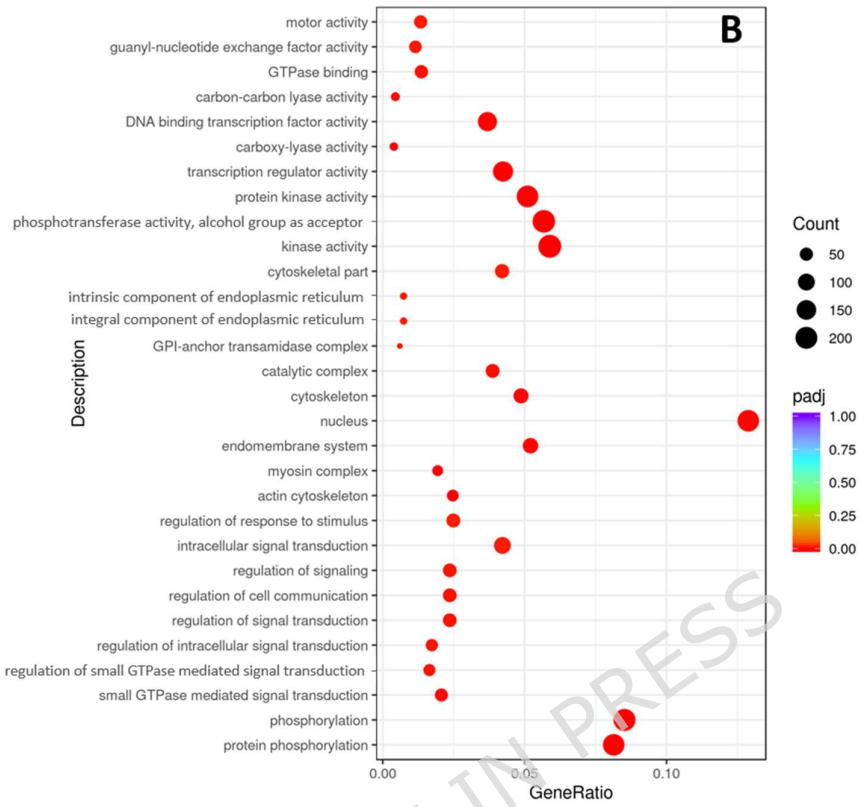

Fig. 4B

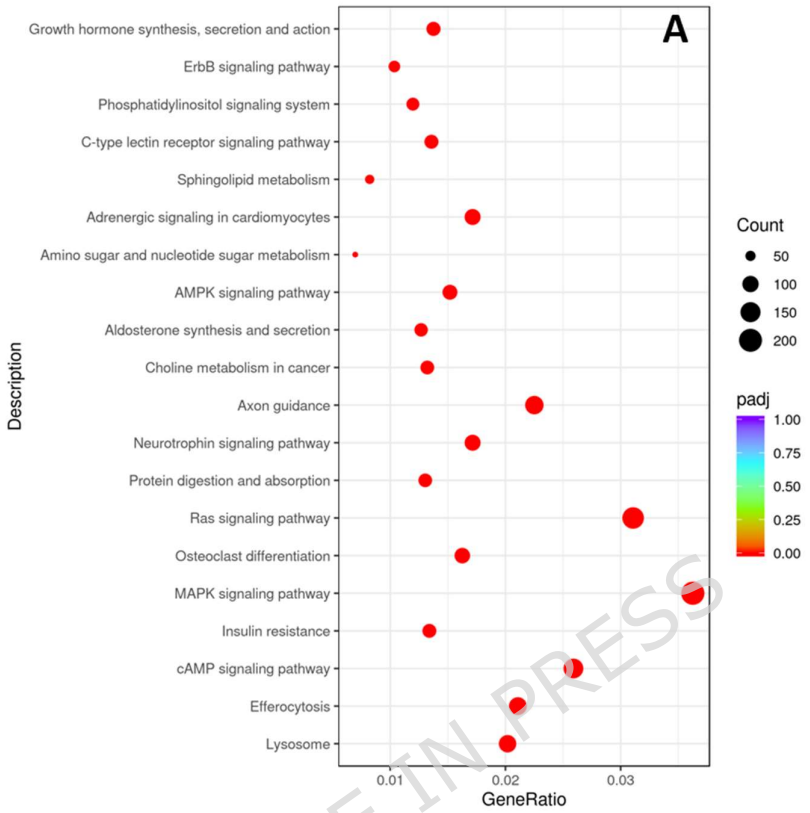

Fig. 5A

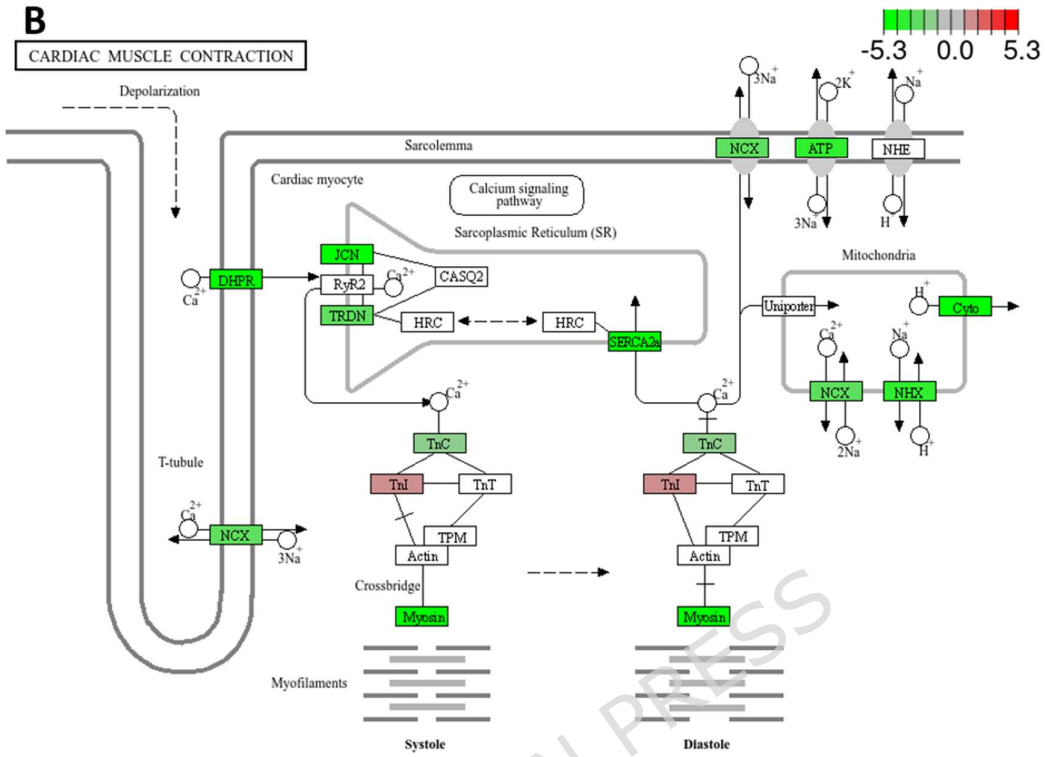

Fig. 5B

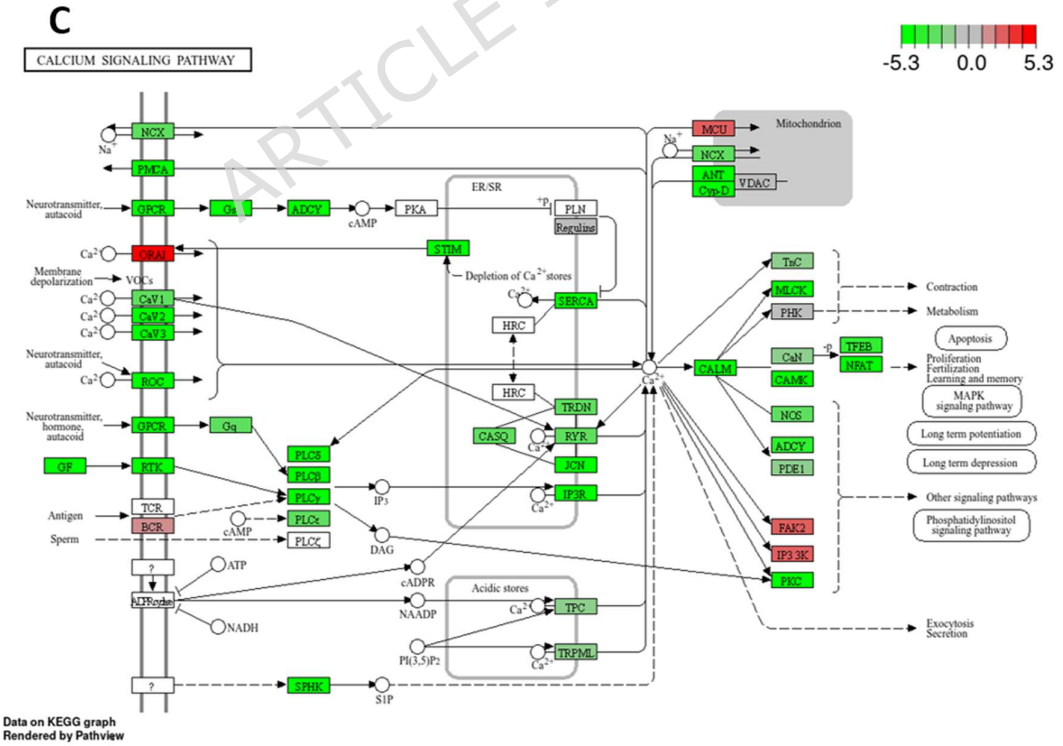

Fig. 5C

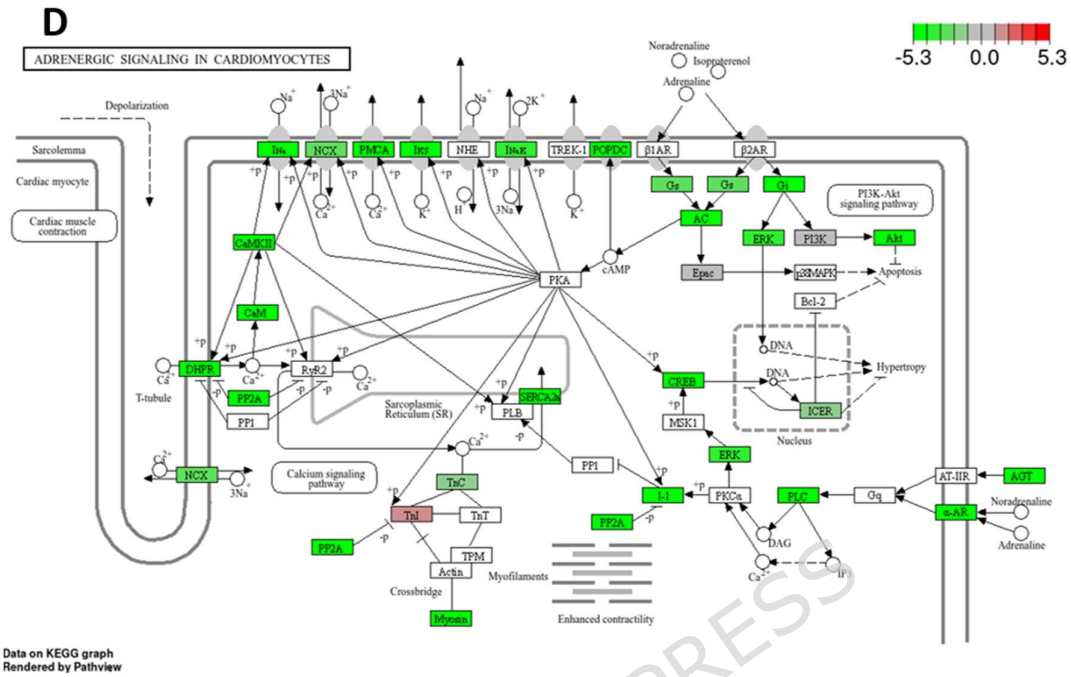

Fig. 5D

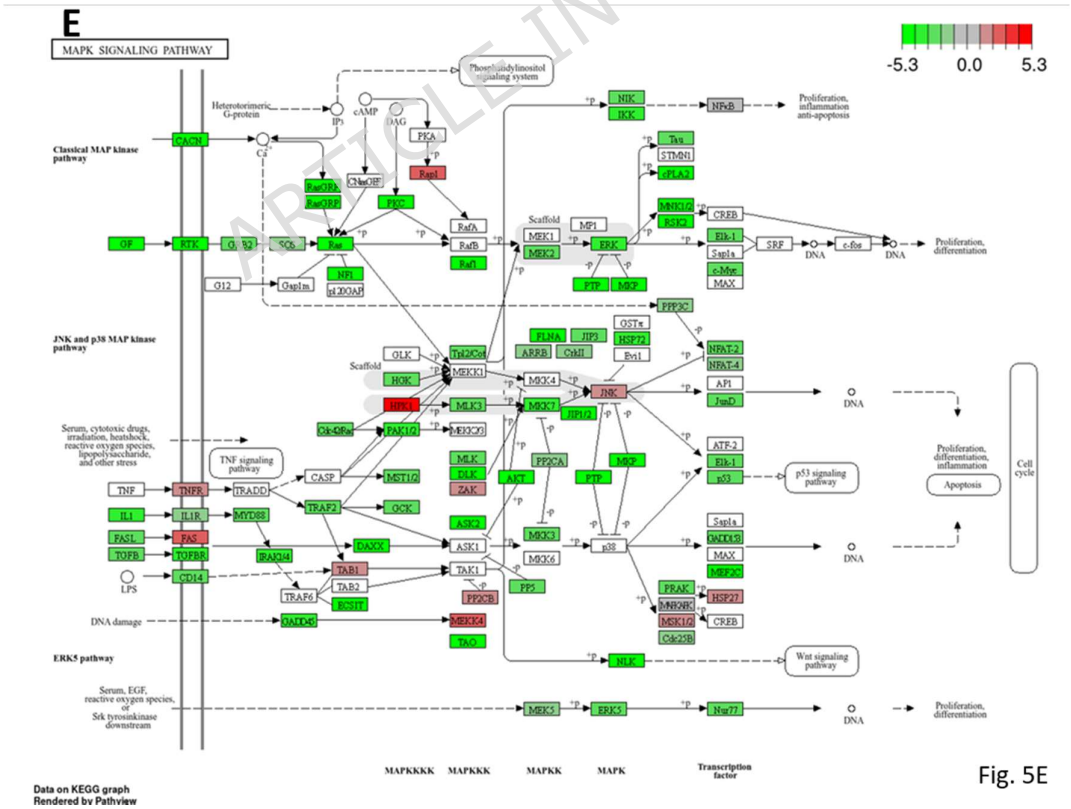

Fig. 5E

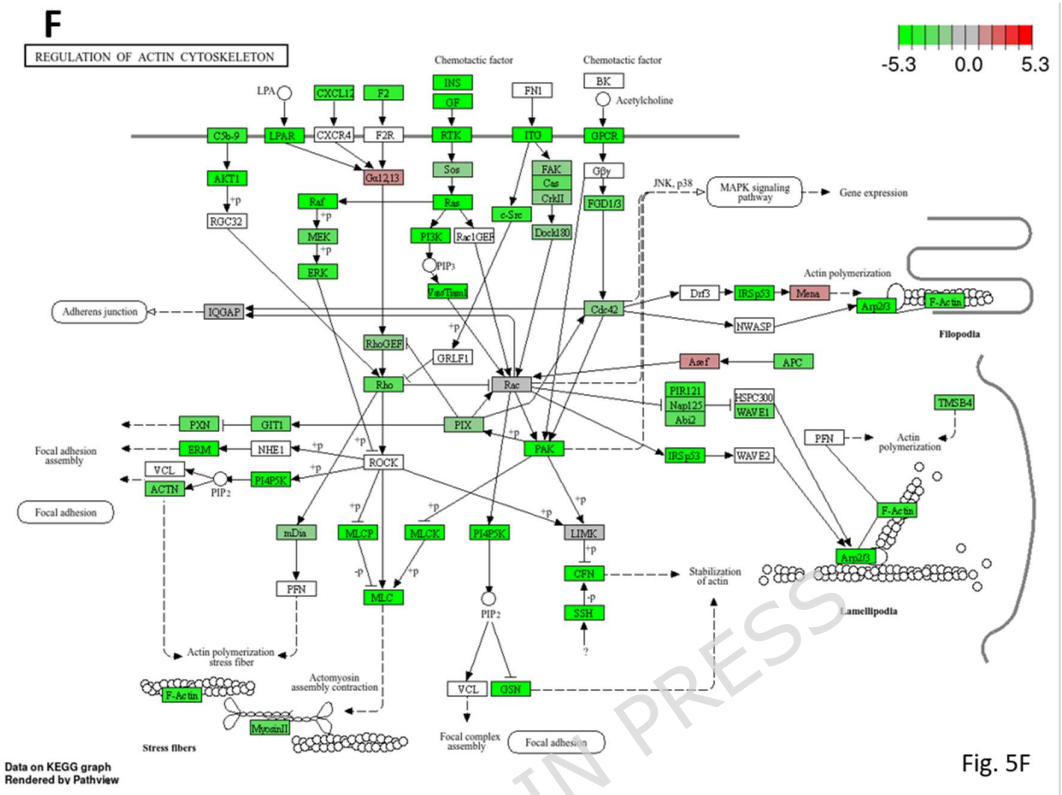

Fig. 5F